

Accuracy of Legendre Moments for Image Representation

Cesar Bustacara-Medina

Department of Systems Engineering
Pontificia Universidad Javeriana
Bogotá D.C., Colombia
cbustaca@javeriana.edu.co

Enrique Ruiz-García

Department of Systems Engineering
Pontificia Universidad Javeriana
Bogotá D.C., Colombia
eruib@javeriana.edu.co

ABSTRACT

Existing works on orthogonal moments are mainly focused on optimizing classical orthogonal Cartesian moments, such as Legendre moments, Gauss-Hermite moments, Gegenbauer moments, and Chebyshev moments. Research in this area generally includes accurate calculation, fast computation, robustness/invariance optimization, and the application of orthogonal moments. This paper presents the inclusion of the integration method proposed by Holoborodko to calculate the Legendre moments. The results obtained are compared with the traditional equation and the methods proposed by Hosny and Pawlak to approximate the integration computation.

Keywords

Image Processing, Image Reconstruction, Legendre Moments, Orthogonal Moments, Moments Computation.

1 INTRODUCTION

Image representation is a principal research area in image processing, pattern recognition, and robotics. In general, there are three types of image representation: the first is developed to support special devices; the second is for the compression of images; and the third is developed to support special image operations [1, 2, 3]. Orthogonal moments, such as Legendre moments and Zernike moments, were first introduced in image processing by Teague [4] and they have been widely used in image analysis and pattern recognition [5, 6] due to their near-zero information redundancy and high discriminative power. Moment-based image representation has been reported to be effective in satisfying the core conditions of semantic description due to its beneficial mathematical properties, especially geometric invariance and independence [1]. For example, moment functions of image intensity values have been successfully used in object recognition [5, 7, 8, 9, 10], image analysis [4, 11, 12, 13, 14], object representation [15], edge detection [16, 17, 18], and texture analysis [19].

Moments and invariant moments were introduced to the pattern recognition community in 1962 by Hu [10]. Since then, after almost 60 years of research, numerous moment-based techniques have been developed for image representation with varying success

degrees. For example, researchers has been introduced Invariant Moments, Rotational Moments, Orthogonal Moments, Complex Moments, and Standard Moments [1, 20]. In 1998, Mukundan and Ramakrishnan [21] surveyed the main publications proposed until then and summarized the theoretical aspects of several classical moment functions. In 2006, Pawlak [12] gave a comprehensive survey on the reconstruction and calculation aspects of the moments with great emphasis to the accuracy/error analysis. In 2007, Shu et al. [22, 23, 24] provided a brief literature review for the mathematical definitions, invariants, and fast/accurate calculations of the classical moments, respectively. In 2009, Flusser et al. [25] presented an overview of moment-based pattern recognition methods with significant contribution to the theory of invariant moments. The substantial expansion [26] of this book includes more detailed analysis of the 3D object invariant representation. In 2011, Hoang [27] reviewed unit disk-based orthogonal moments in his doctoral dissertation, covering theoretical analysis, mathematical properties, and specific implementation. For most of the above reviews, state-of-the-art methods in the past 10 years are not covered. In 2014, Papakostas et al. [28] gave a global overview of the milestones in the 50 years research and highlighted all recent rising topics in this field. However, the theoretical basis for these latest research directions is rarely introduced. In 2019, Kaur et al. [29] provided a comparative review for many classical and new moments. More recently, in 2023, Qi et al. [1] provided a comprehensive survey of the orthogonal moments for image representation, covering recent advances in fast/accurate calculation, robustness/invariance optimization, definition extension, and their application.

Permission to make digital or hard copies of all or part of this work for personal or classroom use is granted without fee provided that copies are not made or distributed for profit or commercial advantage and that copies bear this notice and the full citation on the first page. To copy otherwise, or republish, to post on servers or to redistribute to lists, requires prior specific permission and/or a fee.

Orthogonal moments are shown to be less sensitive to noise and have an efficient capability to feature representation. They allow to reconstruct the image intensity function analytically, from a finite set of moments, using the inverse moment transform [30]. Legendre and Zernike moments are most widely used because their minimum redundancy. Indeed, they can represent the properties of an image with no redundancy or overlap information between the moments. Unfortunately, these approaches are often characterized by a huge computational complexity, making them unsuitable for real-time applications. This lead many researchers to develop faster and accurate algorithms for computing Legendre and Zernike moments [31]. Specifically, the computation of Legendre moments is in general a time consuming process. In many references [32, 33, 34], their computation has been performed using closed form representations for orthogonal polynomials, and taking little care to the accuracy of the quadrature formulas used to approximate integrals.

In general, the calculation of orthogonal moments suffers from geometric error, numerical integration error, and representation error (mainly numerical instability). These errors will severely restrict the quality of image representation, especially when high-order moments are required to better image description. According to Qi et al. [1], the accurate computation strategies of moments are vital for their applicability.

The rest of the paper is organized as follows: In Section 2, an overview of Legendre moments is given. The accuracy computation of Legendre Moments is described in Section 3. Section 4 presents an experimental results of the different methods used to compute Legendre Moments, including the Holoborodko method that is proposed in this paper. Conclusions are presented in Section 5.

2 LEGENDRE MOMENTS

Legendre moments suggested by Teague [4] are one of the important continuous orthogonal moments defined in a rectangular region and have been well researched since the early years of moment-based descriptor studies [4, 14, 35, 36, 37]. In general, Legendre moments form an orthogonal set, defined in Cartesian coordinate space [21, 38] and have been used to analyze and extract features, for example, in facial recognition, image indexing, pattern recognition, etc.

Legendre moments usually contain Legendre polynomials as the kernel which approximated by sampling at fixed intervals, so, the resulted moments have approximated values. In Addition, Legendre moments are orthogonal and scale invariants hence they are suitable for representing the features of the images [39]. In this case, the image intensity distribution can be analytically reconstructed from its orthogonal moments.

2.1 Definitions and Properties

The kernel of Legendre moments are products of Legendre polynomials defined along rectangular image coordinate axes inside a unit circle [3, 4, 21, 38, 40]. The Legendre moments of order $(p + q)$ are defined as

$$L_{pq} = \frac{(2p+1)(2q+1)}{4} \int_{-1}^1 \int_{-1}^1 P_p(x)P_q(y) f(x,y) dx dy \quad (1)$$

where the functions $P_p(x)$ and $P_q(y)$ denote Legendre polynomial of order p and q , respectively. The Legendre moments L_{pq} generalizes the geometric moments m_{pq} , in the sense that the monomial $x^p y^q$ is replaced by the orthogonal polynomial $P_p(x)P_q(y)$ of the same order.

In order to evaluate the Legendre moments, the image coordinate space has to be necessarily scaled so that their respective magnitudes are less than 1. If the image dimension along each coordinate axis is N pixels, and i, j denote the pixel coordinate indices along the axes, then $0 \leq i, j \leq N$, and the discrete version of the Legendre moments can be written as

$$L_{pq} = \frac{(2p+1)(2q+1)}{(N-1)^2} \sum_{i=1}^N \sum_{j=1}^N P_p(x_i)P_q(y_j) f(i, j) \quad (2)$$

where x_i, y_j denote the normalized pixel coordinates in the range $[-1, 1]$, given by

$$x_i = \left(\frac{2i}{N}\right) - 1; \quad y_j = \left(\frac{2j}{N}\right) - 1 \quad (3)$$

The functions $P_p(x)$ form a complete orthogonal basis set inside the unit circle, and the function $f(i, j)$ can be approximated by a truncated series of Legendre moments as:

$$f(i, j) \cong \sum_p \sum_q L_{pq} P_p(x_i) P_q(y_j) \quad (4)$$

The above equation represents the inverse moment transform used for image reconstruction from a finite set of Legendre moments [3, 38].

Teague [4] derived a simple approximation to the inverse transform for a set of moments through order N . Additionally, Teh and Chin [14] indicated that, if only Legendre moments of order $\leq N$ are given, then the function $f(x, y)$ can be approximated by

$$f(x, y) \cong \sum_{p=0}^N \sum_{q=0}^p L_{p-q, q} P_{p-q}(x) P_q(y) \quad (5)$$

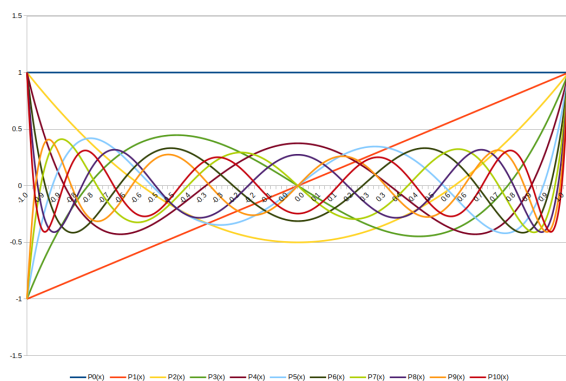


Figure 1: Legendre Polynomials

2.2 Legendre Polynomials

The Legendre polynomials $P_p(x)$ can be given by the equation [40, 41]:

$$P_p(x) = \frac{1}{2^p p!} \frac{d^p}{dx^p} (x^2 - 1)^p \quad (p \geq 0) \quad (6)$$

where $x \in [-1, 1]$, and the Legendre polynomial $P_p(x)$ obeys the following recursive relation [33, 42, 43, 44, 45, 46, 47, 48]:

$$P_{p+1}(x) = \frac{(2p+1)}{(p+1)} x P_p(x) - \frac{p}{(p+1)} P_{p-1}(x) \quad (7)$$

The Eq. (7) also can be rewritten by replacing p with $p-1$ as [2, 21, 35, 49]:

$$P_p(x) = \frac{(2p-1)}{p} x P_{p-1}(x) - \frac{(p-1)}{p} P_{p-2}(x) \quad (8)$$

with $P_0(x) = 1$, $P_1(x) = x$ and $p > 1$. The set of Legendre polynomials $\{P_p(x)\}$ forms a complete orthogonal basis set on the interval $[-1, 1]$.

The plots of the functions $P_p(x)$, with $p = 0, \dots, 10$, are given in Fig. (1).

2.3 Error Analysis

Only in the case of continuous moment functions, their computation over a discrete pixels space (image) is encounters some inaccuracies. These errors are of two types called geometric and numerical errors [1, 50]. The first type of error is caused by the projection of a square discrete image onto the domain (e.g. the unit disc for the radial polynomials) of the polynomial basis, while the numerical error is generated due to the calculation of the double integral over fixed sampling intervals. This case is presented by Papakostas [28] when zeroth-order approximation (ZOA) is applied.

Several approaches have been proposed in the literature towards the minimization of both error types. More

precisely, the geometric errors are minimized by applying specific mapping techniques from the image space to the polynomials domain and appropriate pixels arrangement methodologies [50]. The numerical integration errors are decreased by applying either analytical or approximate iterative integration algorithms (e.g. Simpson, Gauss) [50, 51, 52]. Currently, by using the aforementioned techniques, the values of the derived moments are very close to their theoretical values and, therefore, the level of accuracy achieved is satisfactory [28]. The following section presents the techniques that will be used to analyze the accuracy in the Legendre moments computation and, therefore, in the image reconstruction.

3 ACCURACY COMPUTATION OF LEGENDRE MOMENTS

Liao [36] indicated that the problem of the discretization error for moment computing has been barely investigated though some initial studies into this direction for the case of geometric moments were performed by Teh and Chin [14]. In addition Liao, presents a significant improvement on image reconstructions using Legendre and Zernike Moments. The numerical integration error is decreased by applying either analytical or approximate iterative integration algorithms [40, 50, 51, 52]. Currently, by using classic Newton-Cotes formulas such as Trapezoid, Simpson's, Extended Simpson's, Simpson's 3/8 and Boole's, the derived moment values are very close to their theoretical values and thus, the achieved accuracy level. However, the accuracy in the signals reconstruction (1D, 2D or 3D) is an important challenge today. For example, Table (1) shows the degree, formula, and error term of the classical Newton-Cotes techniques. Specifically, the accuracy degree is the largest positive integer that gives an exact value for x^k , for every k -value.

In addition, approximated Legendre moments defined by Eq. (1) are not accurate, where the double integration is replaced by double summation. Based on the basis of mathematical analysis, double summation is identical to the double integration only when the indices are reaching to infinity. In computing environment, this is not possible [51].

Generalizing, a digital image of size $M \times N$ is an array of pixels. Centers of these pixels are the points (x_i, y_j) , where the image intensity function is defined only for this discrete set of points $(x_i, y_j) \in [-1, 1] \times [-1, 1]$. Where $\Delta x_i = x_{i+1} - x_i$, and $\Delta y_j = y_{j+1} - y_j$ are sampling intervals in the x - and y -directions respectively. In the literature of digital image processing, the intervals Δx_i and Δy_j are fixed at constant values $\Delta x_i = 2/M$, and $\Delta y_j = 2/N$, respectively. Therefore, the points (x_i, y_j) will be defined as follows [40, 51]:

Integration Technique	Degree	Step Size (Δx)	Formula	Error Term
Trapezoid	1	$b - a$	$\frac{\Delta x}{2} (f_0 + f_1)$	$-\frac{1}{12} (\Delta x)^3 f^{(2)}(\xi)$
Simpson's	2	$\frac{b-a}{2}$	$\frac{\Delta x}{3} (f_0 + 4f_1 + f_2)$	$-\frac{1}{90} (\Delta x)^5 f^{(4)}(\xi)$
Simpson's 3/8	3	$\frac{b-a}{3}$	$\frac{3\Delta x}{8} (f_0 + 3f_1 + 3f_2 + f_3)$	$-\frac{3}{80} (\Delta x)^5 f^{(4)}(\xi)$
Boole's	4	$\frac{b-a}{4}$	$\frac{2\Delta x}{45} (7f_0 + 32f_1 + 12f_2 + 32f_3 + 7f_4)$	$-\frac{8}{945} (\Delta x)^7 f^{(6)}(\xi)$

Table 1: Newton-Cotes techniques

$$x_i = -1 + \left(i - \frac{1}{2}\right) \Delta x_i, \quad y_j = -1 + \left(j - \frac{1}{2}\right) \Delta y_j \quad (9)$$

With $i = 1, 2, 3, \dots, M$, and $j = 1, 2, 3, \dots, N$. Eq. (2) could be rewritten as follows:

$$L_{pq} = \frac{(2p+1)(2q+1)}{(M-1)(N-1)} \sum_{i=1}^M \sum_{j=1}^N P_p(x_i) P_q(y_j) f(i, j) \quad (10)$$

Eq. (10) is so-called direct method for Legendre moments computations, which is the approximated version using zeroth-order approximation (ZOA). As were indicated by Liao and Pawlak [37], Eq. (10) is not a very accurate approximation of Eq. (1).

Therefore, to improve the accuracy, in 1996, Liao and Pawlak [37] proposed to use the following approximated form:

$$L_{pq} = \frac{(2p+1)(2q+1)}{4} \sum_{i=1}^M \sum_{j=1}^N h_{pq}(x_i, y_j) f(x_i, y_j) \quad (11)$$

where

$$h_{pq}(x_i, y_j) = \int_{x_i - (\Delta x_i/2)}^{x_i + (\Delta x_i/2)} \int_{y_j - (\Delta y_j/2)}^{y_j + (\Delta y_j/2)} P_p(x) P_q(y) dx dy \quad (12)$$

Liao and Pawlak proposed the Alternative Extended Simpson's Rule (AESR) method to evaluate the double integral defined by Eq. (12), and then they use it to calculate the Legendre moments defined by Eq. (11). AESR method is shown in Eq. (13).

$$\int_a^b f(x) dx \cong \frac{h}{48} [17f_0 + 59f_1 + 43f_2 + 49f_3 + 48 \sum_{i=4}^{n-4} f_i + 49f_{n-3} + 43f_{n-2} + 59f_{n-1} + 17f_n] \quad (13)$$

Then, in 2005, Yap and Paramesran [39] indicated that the approximation of the integral terms in Eq. (12)

is responsible for the approximation error of Legendre moments. These integrals need to be evaluated exactly to remove the approximation error of the Legendre moments computation and they proposed a method to compute the exact values of the Legendre moments by mathematically integrating the Legendre polynomials over the corresponding intervals of the image pixels. In 2007, Hosny [40] proposed a new accurate and fast method for exact Legendre moments computation. The set of Legendre moment can be computed exactly by:

$$L_{pq} = \sum_{i=1}^M \sum_{j=1}^N I_p(x_i) I_q(y_j) f(x_i, y_j) \quad (14)$$

where

$$I_p(x_i) = \frac{(2p+1)}{(2p+2)} [x P_p(x) - P_{p-1}(x)]_{U_i}^{U_{i+1}} \quad (15)$$

$$I_q(y_j) = \frac{(2q+1)}{(2q+2)} [y P_q(y) - P_{q-1}(y)]_{V_j}^{V_{j+1}} \quad (16)$$

This kernel is independent of the image. Therefore, this kernel can be pre-computed, stored and recalled whenever it is needed to avoid repetitive computation.

In 2011, Holoborodko [53] indicated that there are several ways on how to improve high-order Newton-Cotes formulas. The most obvious is to re-target some of the degrees of freedom in the system from contributing to highest approximating order to regularization and stronger noise suppression. Natural way of doing this is to use least squares approximation instead of interpolation. On the contrary to interpolation, least squares make possible to derive several integration filters of the same approximation order. Table (2) shows the formulas derived by Holoborodko of $O(h^5)$ and $O(h^7)$ [53]. In this paper, the formula of order 9 will be used seeking to obtain a greater accuracy in the numerical integration.

In general, given the large number of possible ways to compute the integrals associated with the Legendre moments, in this paper is proposed to use the Holoborodko formula of order 9. In addition, it is compared with a traditional one (Composite Simpson's 1/3 rule), AESR proposed by Pawlak, and the one proposed by Hosny.

N	Stable/Low Noise Newton-Cotes Formulas of $O(h^5 f^{(4)})$ and $O(h^7 f^{(6)})$	Error Term
5	$\frac{4\Delta x}{105} (11f_0 + 26f_1 + 31f_2 + 26f_3 + 11f_4)$	$\frac{34(\Delta x)^5}{315} f^{(4)}(\xi)$
6	$\frac{5\Delta x}{336} (31f_0 + 61f_1 + 76f_2 + 76f_3 + 61f_4 + 31f_5)$	$\frac{265(\Delta x)^5}{1008} f^{(4)}(\xi)$
7	$\frac{\Delta x}{14} (7f_0 + 12f_1 + 15f_2 + 16f_3 + 15f_4 + 12f_5 + 7f_6)$	$\frac{39(\Delta x)^5}{70} f^{(4)}(\xi)$
7	$\frac{\Delta x}{770} (268f_0 + 933f_1 + 786f_2 + 646f_3 + 786f_4 + 933f_5 + 268f_6)$	$\frac{17(\Delta x)^7}{308} f^{(6)}(\xi)$
8	$\frac{7\Delta x}{31680} [1657(f_0 + f_7) - 5157(f_1 + f_6) + 4947(f_2 + f_5) + 4079(f_3 + f_4)]$	$\frac{11767(\Delta x)^7}{6400} f^{(6)}(\xi)$
9	$\frac{8\Delta x}{6435} [309(f_0 + f_8) + 869(f_1 + f_7) + 904(f_2 + f_6) + 779(f_3 + f_5) + 713f_4]$	$\frac{2696(\Delta x)^7}{1971200} f^{(6)}(\xi)$

Table 2: Newton-Cotes Formulas derived by Holoborodko

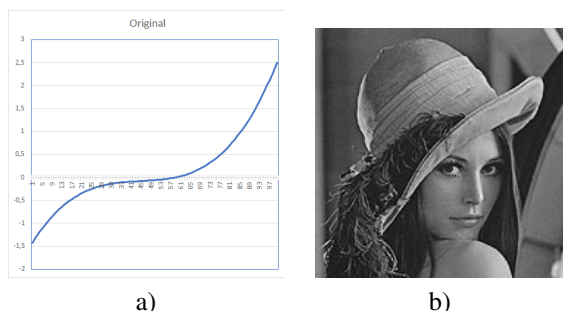


Figure 2: Testing data. a) unidimensional signal b) lena image

4 EXPERIMENTAL RESULTS

To compare the reconstructed signals and images with the originals, here is adopted the Mean Square Error (MSE) and the Peak Signal to Noise Ratio (PSNR) as the measurements, which are signal or image independent and can be used to evaluate the reconstruction signal performance [36]. PSNR is the ratio between the maximum power of the signal and the affecting noise, and is defined as

$$PSNR = 10 \log_{10} \left(\frac{G_{Max}^2}{MSE} \right) \quad (17)$$

where G_{Max}^2 is the maximum value of the signal or gray level of the image, which is 255 in our case, and MSE is defined by

$$MSE = \frac{1}{MN} \sum_{i=1}^M \sum_{j=1}^N |f(x_i, y_j) - \hat{f}(x_i, y_j)|^2 \quad (18)$$

Figure (2) shows the test data (signal and image) used in this paper. The signal is artificially constructed, while the image (Lena) is taken from the traditional images used in digital image processing. The image resolution is 170x170 and has 256 gray levels.

First, the reconstruction of the one-dimensional signal shown in Fig. (2)a is carried out using the different integration techniques mentioned. Signal reconstruction

is generated by varying the number of Legendre Moments and for each of them the MSE and PSNR are calculated respectively. The results obtained from MSE and PSNR for the signal using the four integration techniques to calculate the Legendre moments are shown in Fig. (3). In Fig. 3a can be seen that the values for MSE are very similar and have a decreasing behavior and tend to zero, which implies a good signal reconstruction. Regarding the PSNR, Fig. 3b shows that the best result corresponds to the Hosny technique. Additionally, it can be seen that the four techniques reach a stable state from the fifth order of the Legendre Moments.

Fig. (4) shows the reconstructed signals using five Legendre moments. The original signal is also presented to compare the behavior of the integration techniques and the reconstructed signal from the computation of the Legendre moments. It can be concluded that the reconstructed signals present a high precision with respect to the original signal. However, the biggest error corresponds to the AESR-based technique, which generates differences in the initial part of the reconstruction. The ZOA, Holoborodko and Hosny techniques present better precision in the reconstructed signal.

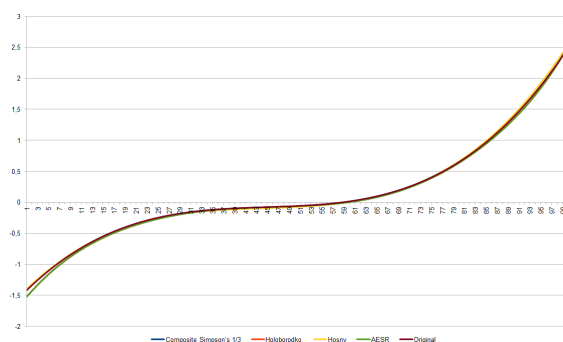


Figure 4: Signal reconstruction.

Regarding image reconstruction, Fig. (5) shows the results of MSE and PSNR. It can be observed that the behavior of the MSE is decreasing for the four techniques applied in the first 90 Legendre Moments, however, this situation begins to change for the Holoborodko, AESR

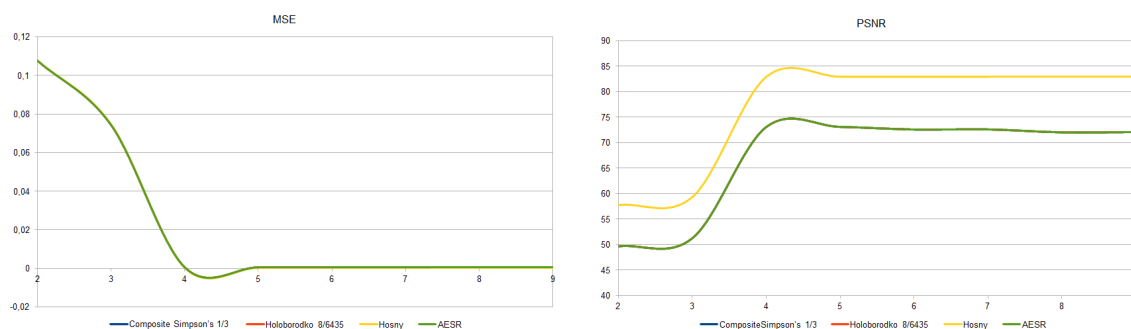


Figure 3: MSE and PSNR for one-dimensional signal.

and Composite Simpson 1/3 techniques. These techniques become unstable and increasing, generating possible results of low precision in the image reconstruction. For its part, the technique proposed by Hosny keeps the MSE decreasing and with a tendency to stabilization, from the Legendre Moment 160, approximately.

Fig. (5) also presents the PSNR behavior for Lena image, where it can be seen that the stability of the technique proposed by Hosny is high, regardless of the order of the Legendre Moments degree. For its part, the PSNR precision using the other techniques (AESR, ZOA and Holoborodko) is reduced from order 90, which implies a possible reduction in the image reconstruction accuracy.

In Fig. (6) three images reconstructed by each of the techniques used (ZOA, AESR, Holoborodko, and Hosny) are presented. Images reconstruction were calculated using Legendre Moments with order between 10 and 300 with steps of 10. Based on the behavior of the MSE and the PSNR, those of order 90, 100 and 110 were selected (see Fig. (5)). As can be seen for the different orders, the images present accuracy problems, mainly at the edges, where pixels with incorrect gray levels appear. Additionally, for the order 110, the accuracy problems are resolved in all cases, but the MSE and PSNR values are better for the Hosny technique. In the particular case of Holoborodko technique, it can be observed that it presents good results, but it does not exceed those obtained using the technique proposed by Hosny.

5 CONCLUSIONS

For the computation of Legendre Moments there are different techniques with different levels of precision. The use of the numerical integration formulas for uniformly spaced data proposed by Holoborodko, derived from the stable Newton-Cotes quadrature rules that are based on the least squares approximation instead of interpolation, was proposed. The Holoborodko technique was compared with respect to techniques such as ZOA, AESR and the one proposed by Hosny, reaching satisfactory results. The results were better than using ZOA

and AESR, but it is necessary to continue exploring the Holoborodko technique using more test images to obtain conclusive information about its strengths and weaknesses. In future works it is necessary to identify the causes of loss of precision after a certain order of the Legendre Moments, because initially it can be seen that precision is lost since many values of the orthogonal product of the legendre polynomials become close to zero. This causes deterioration in the reconstructed images, as can be seen in the MSE and PSNR figures.

6 REFERENCES

- [1] S. Qi, Y. Zhang, C. Wang, J. Zhou, and X. Cao, "A Survey of Orthogonal Moments for Image Representation: Theory, Implementation, and Evaluation," *ACM Computing Surveys*, vol. 55, no. 1, pp. 1–35, jan 2023.
- [2] W. Huang, C. Chen, M. Sarem, and Y. Zheng, "Overlapped rectangle Image representation and its application to exact Legendre moments computation," *Geo-Spatial Information Science*, vol. 11, no. 4, pp. 294–301, dec 2008.
- [3] R. Mukundan and K. R. Ramakrishnan, "FAST COMPUTATION OF LEGENDRE AND ZERNIKE MOMENTS," *Pattern Recognition*, vol. 28, no. 9, pp. 1433–1442, 1995.
- [4] M. R. Teague, "Image Analysis Via the General Theory of Moments." *Journal of the Optical Society of America*, vol. 70, no. 8, pp. 920–930, 1980.
- [5] S. H. Abdhussain, B. M. Mahmmmod, A. Al-Ghadhban, and J. Flusser, "Face Recognition Algorithm Based on Fast Computation of Orthogonal Moments," *Mathematics*, vol. 10, no. 15, aug 2022.
- [6] L. Maofu, H. Yanxiang, and Y. Bin, "Image Zernike moments shape feature evaluation based on image reconstruction," *Geo-Spatial Information Science*, vol. 10, no. 3, pp. 191–195, 2007.
- [7] C.-H. Lo and H.-S. Don, "3-D moment forms: Their construction and application to object

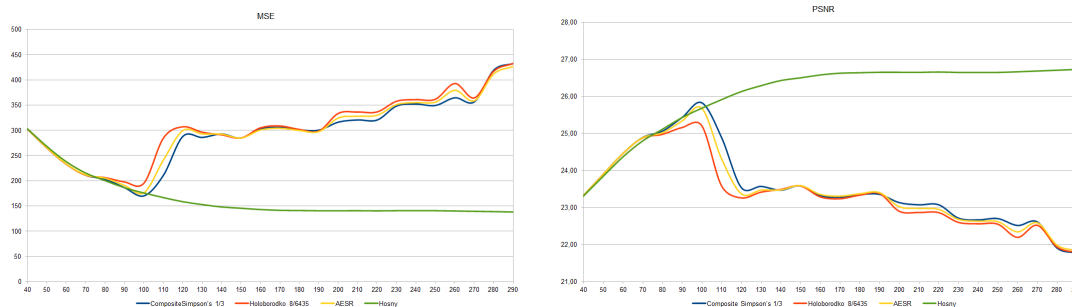


Figure 5: MSE and PSNR for two-dimensional signal (image).

Moment	Comp. Simpson's 1/3	Holoborodko	AESR	Hosny
90				
100				
110				

Figure 6: Reconstructed images from different Legendre moments orders.

identification and positioning,” *Pattern Analysis and Machine Intelligence*, vol. 11, no. 10, pp. 1053–1064, 2002. [Online]. Available: http://ieeexplore.ieee.org/xpls/abs_all.jsp?arnumber=42836

[8] J. Flusser and T. Suk, “Pattern recognition by affine moment invariants,” *Pattern Recognition*, vol. 26, no. 1, pp. 167–174, 1993.

[9] S. A. Dudani, K. J. Breeding, and R. B. McGhee, “Aircraft Identification by Moment Invariants,” *IEEE Transactions on Computers*, vol. C-26, no. 1, pp. 39–46, 1977.

[10] M. K. Hu, “Visual Pattern Recognition by Moment Invariants,” *IRE Transactions on Information Theory*, vol. 8, no. 2, pp. 179–187, 1962.

[11] M.W. Nasrudin, N. S. Yaakob, N. A. Abdul Rahim, M. Z. Zahir Ahmad, N. Ramli, and M. S. Aziz Rashid, “Moment Invariants Technique for Image Analysis and Its Applications: A Review,” in *Journal of Physics: Conference Series*, vol. 1962, no. 1. IOP Publishing Ltd, jul 2021.

[12] M. Pawlak, “Image Analysis by Moments: Reconstruction and Computational Aspects,” Ph.D. dissertation, 2006.

[13] X. S. Liao, “Image Analysis by Moments,” Ph.D. dissertation, 1993.

[14] C. H. Teh and R. T. Chin, “On image analysis by the methods of moments,” *IEEE Transactions on Pattern Analysis and Machine Intelligence*, no. December, pp. 556–561, 1988.

[15] R. C. Papademetriou, “Reconstructing with moments,” in *Proceedings - International Conference on Pattern Recognition*, 1992, pp. 476–480.

[16] L.-M. Luo, X.-H. Xie, and X.-D. Bao, “A Modified Moment-Based Edge Operator for Rectangular Pixel Image,” *IEEE Transactions on Circuits*

- and Systems for Video Technology, vol. 4, no. 6, pp. 552–554, 1994.
- [17] S. Ghosal and R. Mehrotra, “Orthogonal Moment Operators for Subpixel Edge Detection,” *Pattern Recognition*, vol. 26, no. 2, pp. 295–306, 1993.
- [18] L. M. Luo, C. Hamitouche, J. L. Dillenseger, and J. L. Coatrieux, “A Moment-Based Three-Dimensional Edge Operator,” *IEEE Transactions on Biomedical Engineering*, vol. 40, no. 7, 1993.
- [19] M. Tuceryan, “Moment based texture segmentation,” in *Proceedings - International Conference on Pattern Recognition, 1992*, pp. 45–48.
- [20] R. J. Prokop and A. P. Reeves, “A survey of moment-based techniques for unoccluded object representation and recognition,” *CVGIP: Graphical Models and Image Processing*, vol. 54, no. 5, pp. 438–460, 1992.
- [21] R. Mukundan and K. R. Ramakrishnan, “Legendre Moments,” in *Moment Functions in Image Analysis: Theory and Applications*. World Scientific Publishing, 1998, ch. 4, pp. 49–56.
- [22] H. Shu, L. Luo, and J.-L. Coatrieux, “Moment-based approaches in imaging part 3: computational considerations,” *IEEE Engineering in Medicine and Biology Magazine*, vol. 27, no. 3, pp. 89–91, 2008.
- [23] —, “Moment-based approaches in imaging part 2: invariance,” *IEEE Engineering in Medicine and Biology Magazine*, vol. 27, no. 1, pp. 81–83, 2008.
- [24] —, “Moment-based approaches in imaging part 1, basic features,” *IEEE Engineering in Medicine and Biology Magazine*, vol. 26, no. 5, pp. 70–74, 2007.
- [25] J. Flusser, T. Suk, and B. Zitová, *Moments and Moment Invariants in Pattern Recognition*. John Wiley Sons, Ltd., 2009.
- [26] —, *2D and 3D Image Analysis by Moments*. John Wiley Sons, Ltd, 2017.
- [27] T. V. Hoang, “Image Representations for Pattern Recognition Image,” Ph.D. dissertation, Université Nancy II, 2011.
- [28] G. Papakostas, “Over 50 Years of Image Moments and Moment Invariants,” in *Moments and Moment Invariants - Theory and Applications*. Science Gate Publishing, 2014, vol. 1, no. July 2014, pp. 3–32.
- [29] P. Kaur, H. S. Pannu, and A. K. Malhi, “Comprehensive study of continuous orthogonal moments-A systematic review,” *ACM Computing Surveys*, vol. 52, no. 4, 2019.
- [30] C. D. Ruberto, L. Putzu, and G. Rodriguez, “Fast and accurate computation of orthogonal moments for texture analysis,” *Pattern Recognition*, vol. 83, pp. 498–510, 2018.
- [31] S. K. Hwang and W. Y. Kim, “A novel approach to the fast computation of Zernike moments,” *Pattern Recognition*, vol. 39, no. 11, pp. 2065–2076, 2006.
- [32] B. Vijayalakshmi and V. Subbiah Bharathi, “Classification of CT liver images using local binary pattern with Legendre moments,” *Current Science*, vol. 110, no. 4, pp. 687–691, 2016.
- [33] M. Oujoura, B. Minaoui, and M. Fakir, “Image Annotation by Moments,” in *Moments and Moment Invariants - Theory and Applications*, jul 2014, ch. 10, pp. 227–252.
- [34] K. Wu, C. Garnier, J. L. Coatrieux, and H. Shu, “A preliminary study of moment-based texture analysis for medical images,” in *2010 Annual International Conference of the IEEE Engineering in Medicine and Biology Society, EMBC’10*, no. 1, 2010, pp. 5581–5584.
- [35] A. N. Hashimi and B. N. Kadhim, “Face recognition based on fusion of SVD and Legendre moment,” in *Journal of Physics: Conference Series*, vol. 1530, no. 1. Institute of Physics Publishing, may 2020.
- [36] S. Liao, “Accuracy Analysis of Moment Functions,” in *Moments and Moment Invariants - Theory and Applications*. Science Gate Publishing, jul 2014, ch. 2, pp. 33–56.
- [37] S. X. Liao and M. Pawlak, “On image analysis by moments,” *IEEE Transactions on Pattern Analysis and Machine Intelligence*, vol. 18, no. 3, pp. 254–266, 1996.
- [38] R. Mukundan, S. H. Ong, and P. A. Lee, “Discrete vs. continuous orthogonal moments for image analysis,” *CISST’01 International Conference*, no. i, pp. 23–29, 2001. [Online]. Available: <http://ir.canterbury.ac.nz/handle/10092/470>
- [39] P.-T. Yap and R. Paramesran, “An Efficient Method for the Computation of Legendre Moments,” *IEEE Transactions on Pattern Analysis and Machine Intelligence*, vol. 27, no. 12, 2005.
- [40] K. M. Hosny, “Exact Legendre moment computation for gray level images,” *Pattern Recognition*, vol. 40, no. 12, pp. 3597–3605, dec 2007.
- [41] C. J. Bustacara Medina, “Evaluación computacional para calcular los polinomios de Legendre de primera clase,” *Revista Avances en Sistemas e Informática*, vol. 7, no. 2, pp. 131–137, 2010.
- [42] P. Wang, “3-D Image Analysis via Jacobi Moments with GPU-Accelerated Algorithms,” *Tech. Rep.*, 2021.
- [43] I. Khalil, A. Khalil, S. U. Rehman, H. Khalil, R.

- A. Khan, and F. Alam, "Classification of ECG Signals Using Legendre Moments," *International Journal of Bioinformatics and Biomedical Engineering*, vol. 1, no. 3, pp. 284–291, 2015. [Online]. Available: <http://www.aiscience.org/journal/ijbbe><http://creativecommons.org/licenses/by-nc/4.0/>
- [44] P.-J. A. Chiang, "Legendre Moments Explorations via Image Reconstruction," Ph.D. dissertation, 2014.
- [45] G. B. Arfken, H. J. Weber, and F. E. Harris, *Mathematical Methods for Physicists*, 7th ed. Elsevier Inc., 2013.
- [46] I. A. Selezneva, Y. L. Ratis, E. Hernández, J. Pérez-Quiles, and P. Fernández de Córdoba, "A CODE TO CALCULATE HIGH ORDER LEGENDRE POLYNOMIALS AND FUNCTIONS," *Revista Academica Colombiana de Ciencia*, vol. 37, no. 145, pp. 541–544, 2013.
- [47] G. Yang, H. Shu, C. Toumoulin, G.-N. Han, and L. M. Luo, "Efficient Legendre moment computation for grey level images," *Pattern Recognition*, vol. 39, no. 1, pp. 74–80, 2006. [Online]. Available: <https://hal.archives-ouvertes.fr/hal-00135862>
- [48] T. L. Chow, *Mathematical methods for physicists : A concise introduction*. Cambridge University Press, 2000.
- [49] E. Marengo, E. Robotti, and M. Demartini, "The use of legendre and zernike moment functions for the comparison of 2-D PAGE maps," in *Methods in Molecular Biology*. Humana Press Inc., 2016, vol. 1384, pp. 271–288.
- [50] S. X. Liao and M. Pawlak, "On the accuracy of zernike moments for image analysis," *IEEE Transactions on Pattern Analysis and Machine Intelligence*, vol. 20, no. 12, pp. 1358–1364, 1998.
- [51] K. M. Hosny, "Image representation using accurate orthogonal Gegenbauer moments," *Pattern Recognition Letters*, vol. 32, no. 6, pp. 795–804, 2011. [Online]. Available: <http://dx.doi.org/10.1016/j.patrec.2011.01.006>
- [52] —, "Efficient Computation of Legendre Moments for Gray Level Images," *International Journal of Image and Graphics*, vol. 7, no. 4, pp. 735–747, 2007.
- [53] P. Holoborodko, "Stable Newton-Cotes Formulas," 2011. [Online]. Available: https://www.researchgate.net/publication/316662645_Stable_Newton-Cotes_Formulas